Regional Rainfall Frequency Analysis via Stochastic Storm Transposition

By Larry L. Wilson[1] and Efi Foufoula-Georgiou,[2]
Associate Member, ASCE

Abstract: In a previous study, Foufoula-Georgiou (1989a) investigated a stochastic storm transposition (SST) approach as a possible methodology of assessing the probability of exceedance of extreme precipitation depths over a catchment. The purpose of this paper is to report further methodological advances on the SST approach and present the results of a pilot implementation study in the Midwest. Under the assumptions of an elliptical storm shape and spread function of a given functional form, extreme storms have been described by the joint probability distribution of seven storm parameters (five specifying the magnitude, orientation, shape, and within-storm spatial variability, and two specifying the location of the storm center). A nonhomogeneous spatial multivariate point process model has been postulated for the joint probability distribution of the storm center depth and storm location and it has been fitted to 65 extreme storms in the nine-state midwestern region. The method has been used to estimate the tails of the probability distribution of the average catchment depths over several hypothetical catchments in the Midwest and to describe the spatial variability of the estimates over the studied region.

Introduction

Several studies have demonstrated that risk-based decision making in water resources, e.g., the selection among alternative spillway designs of new dams or the modification of existing ones, is sensitive to the specification of the risk of very low-frequency events [return period greater than 100 years; see, e.g., Stedinger and Grygier (1985)]. Standard frequency analysis methods do not provide reliable estimates of such low-frequency events and alternative methods need to be developed.

Estimation of the frequency distribution of extreme precipitation depths over a catchment becomes difficult if one relies only on the few storms that have occurred over that particular catchment. The underlying idea of the stochastic storm transposition (SST) approach [the term coined by Fontaine and Potter (1989)] is the enlargement of the record of storms available for estimation by considering storms that have not occurred over the catchment of interest but that could have occurred over it. This approach leads to storm regionalization and estimation of the joint probability distribution of storm characteristics and storm occurrences within a prespecified storm transposition area.

The concept of storm transposition has been extensively used in a deterministic framework for the derivation of probable maximum precipitation (PMP) estimates [e.g., Myers (1967); Wang (1984)] but it has not been adequately explored in a probabilistic framework. Studies on this approach include those of Alexander (1963), Gupta (1972), Newton (1983), Foufoula-

[1]Res. Asst., Dept. of Civ. Engrg., FX-10, Univ. of Washington, Seattle, WA 98195.
[2]Assoc. Prof., St. Anthony Falls Hydr. Lab., Dept. of Civ. and Mineral Engrg., Univ. of Minnesota, Minneapolis, MN 55414.

Note. Discussion open until December 1, 1990. To extend the closing date one month, a written request must be filed with the ASCE Manager of Journals. The manuscript for this paper was submitted for review and possible publication on November 22, 1989. This paper is part of the ***Journal of Hydraulic Engineering***, Vol. 116, No. 7, July, 1990. ©ASCE, ISSN 0733-9429/90/0007-0859/$1.00 + $.15 per page. Paper No. 24847.

Georgiou (1989a), and Fontaine and Potter (1989). The discussions prompted by the publication of the paper of Newton are encouraging because they demonstrate that applied hydrologists and meteorologists seem to be in agreement about the necessity of an objective methodology of estimating exceedance probabilities of extreme storms and floods to be used in conjunction with, or as alternatives to, the current PMP/PMF standards of hydraulic design.

The lack of risk estimates prohibits the use of any risk-based economic analysis and decision making in hydraulic design and evaluation of high-hazard dams. This has prompted several investigators [e.g., Buehler (1984)] to suggest the idea of assigning a fixed probability (e.g., 10^{-6} or 10^{-7}) to existing PMP estimates. We are not in agreement with this approach but instead believe that serious efforts have to be directed toward developing a methodology that has an objective basis and can give consistent results of comparative probabilities for a range of extreme rainfall depths and resulting floods (including PMP and PMF estimates). The development of such a methodology has been the motivation of the work presented in Foufoula-Georgiou (1989a) and its extension presented herein. The first paper formulated a probabilistic storm transposition methodology for the estimation of exceedance probabilities of extreme precipitation depths over a catchment and it identified the conceptual and methodological difficulties associated with this approach. In that study, the distribution of extreme storm centers was assumed homogeneous over an arbitrarily selected area and an illustrative implementation considering only 18 very extreme storms in the Midwest was given. The purpose of this paper is to report further methodological advances on the SST approach and present the results of the first pilot implementation study for the Midwest. Also, the results of a preliminary sensitivity analysis of the estimates to uncertainties inherent in the data and estimation procedures are presented. Further refinements of the method and a more extensive sensitivity analysis are currently under study and will be reported in the future.

Brief Review of Stochastic Storm Transposition Approach

Let $d(x,y,t)$ denote the rainfall depth deposited from a storm at the ground location of spatial coordinates (x,y) during a period of time $(0,t]$. For design purposes, a variable of particular interest is the maximum average depth that can occur over a catchment of area A_c during a time period Δt,

$$\bar{d}_c(\Delta t) = \frac{1}{|A_c|}\int\int_{Ac}[d(x,y,t_s+\Delta t) - d(x,y,t_s)]dxdy \quad \ldots\ldots (1)$$

where the period Δt = a critical duration of rainfall in terms of flood production, and

$$t_s = \int\int_{Ac}[d(x,y,t_s+\Delta t) - d(x,y,t_s)]dxdy$$

$$= \int\int_{A_c}[d(x,y,t+\Delta t) - d(x,y,t)]dxdy \;\forall\; t < t_r - \Delta t \quad \ldots\ldots (2)$$

where t_r = the storm duration. The random variable $\bar{d}_c(\Delta t)$ can be interpreted as the maximum average depth deposited from a storm over a catchment of area A_c during a time period equal to Δt.

Following Foufoula-Georgiou (1989a) let Λ_s denote the random vector of storm characteristics describing a storm. In general Λ_s will comprise the parameters of a stochastic model describing the rainfall field. Depending on the model, these parameters may or may not be directly interpretable in terms of physical storm characteristics. Let Λ_p denote the two-dimensional vector describing the position of a storm (here this position is called the storm center). The storm center may be defined as the location of the maximum observed total depth or as the location of the maximum accumulated depth over a specified period of time. Alternatively, it may be defined as the center of mass of the storm. The cumulative distribution function of $\bar{d}_c(\Delta t)$ can be expressed as

$$F_{\bar{d}_c(\Delta t)}(d) = \mathrm{pr}[\bar{d}_c(\Delta t) \le d] \quad \ldots\ldots (3a)$$

$$F_{\bar{d}_c(\Delta t)}(d) = \int_{|\Lambda_s|}\int_{|\Lambda_p|}\mathrm{pr}[\bar{d}_c(\Delta t) \le d|\boldsymbol{\lambda}_s,\boldsymbol{\lambda}_p]dF_{\Lambda_s\Lambda_p}(\boldsymbol{\lambda}_s,\boldsymbol{\lambda}_p) \quad \ldots\ldots (3b)$$

where $F_{\Lambda_s\Lambda_p}(\boldsymbol{\lambda}_s,\boldsymbol{\lambda}_p)$ = the cumulative joint distribution function of the random vectors Λ_s and Λ_p. Of interest is the exceedance probability of $\bar{d}_c(\Delta t)$, which can be obtained as

$$G_{\bar{d}_c(\Delta t)}(d) = 1 - F_{\bar{d}_c(\Delta t)}(d) \quad \ldots\ldots (4)$$

Let $Z(t)$ denote the counting process of the number of extreme storms in an interval of t years (stationarity in time is assumed). The annual exceedance probability can be expressed as

$$G^a_{\bar{d}_c(\Delta t)}(d) = 1 - F^a_{\bar{d}_c(\Delta t)}(d) \quad \ldots\ldots (5a)$$

$$G^a_{\bar{d}_c(\Delta t)}(d) = 1 - \sum_{\nu=0}^{\infty}\mathrm{pr}[\bar{d}_c(\Delta t) \le d|Z(1)=\nu]\cdot\mathrm{pr}[Z(1)=\nu] \quad \ldots\ldots (5b)$$

Assuming that $Z(1)$, the random variable of the number of extreme storm occurrences per year, is independent of the storm depths $\bar{d}_c(\Delta t)$, and that $\bar{d}_c(\Delta t)$ are independent and identically distributed random variables, the annual probability of exceedance of $\bar{d}_c(\Delta t)$ can be written as

$$G^a_{\bar{d}_c(\Delta t)}(d) = 1 - \sum_{\nu=0}^{\infty}[F_{\bar{d}_c(\Delta t)}(d)]^{\nu}\cdot\mathrm{pr}[Z(1)=\nu] \quad \ldots\ldots (6)$$

Assuming that $Z(1)$ follows a Poisson distribution with annual occurrence rate λ (this is a realistic assumption shown later to hold true for Midwestern extreme storms), the annual exceedance probability of $\bar{d}_c(\Delta t)$ can be shown to be

$$G^a_{\bar{d}_c(\Delta t)}(d) = 1 - \exp[-\lambda G_{\bar{d}_c(\Delta t)}(d)] \quad \ldots\ldots (7)$$

Throughout the rest of the paper, $F_{\bar{d}_c(\Delta t)}(d)$ will be abbreviated as $F(d)$ and $F^a_{\bar{d}_c(\Delta t)}(d)$ as $F^a(d)$. $G(d)$ and $G^a(d)$ represent similar abbreviations.

Area of Study and Storm Data Used in Analysis

The area of study is the nine-state Midwestern area of North Dakota, South Dakota, Nebraska, Kansas, Minnesota, Iowa, Missouri, Wisconsin, and Illinois. This area will be referred to as the transposition area, A_{tr}. The data available for the estimation are the extreme storms published in the catalog of the U.S. Army Corps of Engineers (*Storm* 1945–1990). The pros and

cons of using this catalog as the sole source of information for the estimation of the exceedance probabilities of extreme precipitation depths have been discussed in Foufoula-Georgiou and Wilson (1990) and is currently under more detailed investigation. In a preliminary implementation of the SST methodology in the Midwest (Foufoula-Georgiou 1989a), storms were selected from the catalog according to the following two criteria:

1. Their center (defined as the point of maximum total depth) was within the nine-state Midwestern region.
2. Their total 10-sq mi average rainfall depth exceeded 13 in.

These criteria resulted in a total of 18 storms during the 61 years of the available period of storm catalog record for the Midwest (1891–1951). Estimation of the annual exceedance probabilities $G^a(d)$ from only 18 storms proved inadequate, at least in terms of inferring and estimating the spatial storm occurrence process and assessing the probability of very extreme depths of the order of the probable maximum precipitation estimates for the Midwestern region. This prompted the study of Foufoula-Georgiou and Wilson (1990), which was an effort to identify trends and similarities in extreme Midwestern storm characteristics. These results provide the basis of the regional frequency analysis presented in the present paper.

The estimation study reported herein is based on all storms of the catalog that have their centers within the nine-state Midwestern area and for which the maximum recorded 24-hour average depth (Δt = 24 hours) was greater than or equal to 8.0 in. Table 1 identifies and lists 65 such storms, together with their duration, maximum 24-hour observed depth, maximum 24-hour areal extent, and associated average depth reported in the depth-area-duration tables (*Storm* 1945–1990), location, and date of occurrence.

Because of the lack of detailed data for these extreme storms, it was not possible to build a stochastic model that accurately described the space-time structure within the storm. The only data available for estimation are the depth-area-duration (DAD) data, which describe not the actual storm pattern but rather the maximum average depth that can occur over a given area during a given period of time. Note, however, that this maximum average depth over a given area is an important variable in terms of design and its use in design studies is common practice. Due to data limitations, the following assumptions were made regarding the spatial distribution of the maximum 24-hour depth accumulation:

1. The maximum 24-hour depth distribution within the storm area enclosed by the contour of 3 in. (this area is referred to here as the storm area A_s) is described by homocentric, geometrically similar contours around a single center. These contours were further approximated by ellipses of major-to-minor-axis ratio equal to c and orientation of major axis equal to ϕ (this angle being measured counterclockwise from the horizontal east-west direction).
2. The maximum 24-hour average depth over an area A, $[\bar{d}(A)]$, is related to the storm-center depth and the area A by the relationship

$$\bar{d}(A) = d_o e^{-kA^n} \quad (8)$$

where d_o = the maximum 24-hour recorded depth, taken as the storm-center depth, and k and n = parameters to be estimated for each individual storm.

Based on these assumptions, the rainfall depth $d(r, \theta)$ at distance r from

TABLE 1. Characteristics of Extreme Midwestern Storms Used in Analysis

Storm number (1)	U.S. Army Corps of Engineers number (2)	Duration (hours) (3)	Maximum 24-hr depth (in.) (4)	Areal extent sq mi [associated average depth (in.)] (5)	Storm Center		Date (8)
					Town (6)	State (7)	
1	MR 4-24	54	24.0	63,300 (2.7)	Boyden	Iowa	September 1926
2	MR 4-5	20	13.0	20,000 (3.5)	Grant Township	Nebraska	June 1940
3	MR 6-15	78	15.8	16,000 (2.9)	Near Stanton	Nebraska	June 1944
4	MR 7-2A	78	15.0	45,000 (2.9)	Near Cole Camp	Missouri	August 1946
5	MR 1-10	96	14.7	59,000 (2.9)	Woodburn	Iowa	August 1903
6	MR 2-29	78	12.2	113,500 (1.5)	Grant City	Missouri	July 1922
7	MR 1-5	78	12.3	100,000 (2.0)	Primghar	Iowa	July 1900
8	MR 10-2	108	9.3	57,000 (2.5)	Council Grove	Kansas	July 1951
9	MR 8-20	120	12.0	306,000 (0.7)	Near Holt	Missouri	June 1947
10	MR 1-9	168	8.1	136,000 (1.2)	Abilene	Kansas	May 1903
11	MR 3-14	120	8.8	120,000 (2.2)	Pleasanton	Kansas	September 1927
12	MR 4-2	96	12.9	30,000 (2.4)	Larrabee	Iowa	June 1891
13	UMV 1-11	108	11.5	50,000 (2.0)	Ironwood	Michigan	July 1909
14	UMV 2-18	180	8.1	70,000 (1.8)	Boonville	Missouri	September 1905
15	UMV 1-22	78	12.4	60,000 (2.2)	Haywood	Wisconsin	August 1941
16	OR 4-8	90	9.0	70,000 (4.9)	Golconda	Illinois	October 1910
17	SW 2-1	114	14.0	30,000 (2.2)	Near Neosho Falls	Kansas	September 1926
18	MR 1-3A	30	12.5	7,200 (4.1)	Blanchard	Iowa	July 1898
19	MR 2-22	102	11.9	19,900 (2.9)	Warrensburg	Iowa	August 1919
20	MR 4-3	78	12.3	84,000 (1.8)	Greeley	Nebraska	June 1896
21	MR 6-2	96	11.4	16,000 (3.3)	Lindsborg	Kansas	October 1941
22	UMV 3-29	15	12.0	20,000 (2.6)	Near Dumont	Iowa	June 1951
23	GL 2-29	120	12.4	58,000 (2.2)	Near Merrill	Wisconsin	July 1912
24	MR 1-23	96	10.8	40,000 (2.3)	Nemaha	Nebraska	July 1907
25	MR 2-11	96	11.2	24,000 (2.3)	Moran	Kansas	September 1915
26	MR 3-20	60	9.9	60,000 (3.6)	Lebo	Kansas	November 1928
27	UMV 2-5	12	12.1	20,000 (3.9)	Near Bonapart	Iowa	June 1905
28	UMV 2-8	66	8.8	27,000 (3.2)	Bethany	Missouri	July 1909
29	UMV 3-20B	186	8.4	80,000 (2.2)	Galesburg	Illinois	September 1941
30	UMV 3-21	42	11.0	12,600 (2.4)	Thompson Farm	Missouri	July 1942
31	GL 2-12	120	8.9	67,000 (2.4)	Medford	Wisconsin	June 1905
32	UMV 2-14	63	9.6	70,000 (1.6)	Washington	Iowa	June 1930
33	GL 3-11	42	11.0	20,000 (3.2)	Libertyville	Illinois	June 1938
34	MR 1-21A	102	8.6	24,300 (2.7)	Warsaw	Missouri	August 1906
35	MR 3-6	48	8.9	45,000 (2.7)	Lockwood	Missouri	September 1925
36	UMV 2-30	24	11.0	10,400 (2.8)	Oxford Junction	Iowa	June 1944
37	LMV 1-3A	84	8.4	20,000 (3.3)	Sikeston	Missouri	September 1898
38	GL 4-5	66	10.0	15,000 (4.3)	Butternut	Wisconsin	July 1897
39	MR 6-3	24	10.9	5,000 (3.6)	Ballard	Missouri	June 1943
40	MR 1-16A	120	8.2	45,000 (1.7)	El Dorado	Kansas	June 1905
41	MR 6-1	72	8.9	35,000 (2.5)	Clifton Hill	Missouri	June 1942
42	UMV 2-15	24	9.0	13,000 (4.4)	Gorin	Missouri	June 1933
43	UMV 3-28	30	10.7	10,500 (3.8)	Mifflin	Wisconsin	July 1950
44	MR 1-28	78	8.1	39,000 (2.2)	Topeka	Kansas	September 1909
45	MR 3-1A	78	9.0	3,900 (3.9)	Medicine Lodge	Kansas	September 1923
46	MR 3-29	30	10.0	14,000 (3.1)	Sharon Springs	Kansas	May 1938
47	UMV 2-22	30	9.0	23,400 (2.8)	Gunder	Iowa	July 1940
48	UMV 4-11	54	9.2	28,500 (2.3)	Galva	Illinois	August 1924
49	MR 7-9	30	10.0	8,300 (4.1)	Jerome	Iowa	July 1946
50	GL 2-30	54	8.9	5,000 (3.4)	Viroqua	Wisconsin	July 1917
51	MR 3-11	54	8.9	13,300 (2.3)	Chanute	Kansas	April 1927
52	MR 2-23	66	8.7	58,350 (2.6)	Bruning	Nebraska	September 1919
53	MR 4-14A	90	8.5	66,000 (2.3)	Hazelton	North Dakota	June 1914
54	MR 4-12	42	8.4	13,200 (3.7)	Lincoln	Nebraska	August 1910
55	MR 1-3B	30	8.3	20,000 (2.5)	Edgehill	Missouri	July 1898
56	MR 2-3	18	8.0	6,800 (3.9)	Wichita	Kansas	September 1911
57	UMV 1-4A	54	8.0	32,000 (2.1)	Minnesota City	Minnesota	June 1899
58	UMV 2-17	12	8.4	15,000 (2.9)	Toledo	Iowa	August 1929
59	OR 4-22	30	8.0	24,100 (3.6)	Charleston	Illinois	September 1926
60	MR 6-16	36	9.1	5,100 (2.2)	Near Bagnell	Missouri	August 1944
61	MR 7-16	10	10.0	220 (4.3)	Near Gering	Nebraska	June 1947
62	UMV 1-14B	126	8.0	5,000 (2.9)	Worthington	Minnesota	August 1913
63	UMV 1-6	102	8.0	50,000 (3.1)	Elk Point	South Dakota	September 1900
64	UMV 1-7A	78	8.0	15,200 (3.2)	LaCrosse	Wisconsin	October 1900
65	UMV 2-19	3	8.4	570 (2.4)	Plainville	Illinois	May 1941

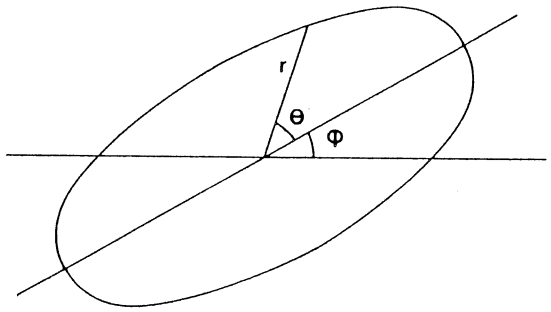

FIG. 1. Elliptical Storm Shape and Definition of Parameters r, θ, and ϕ

the storm center and angle θ from the storm orientation axis (see Fig. 1) is given as

$$d(r,\theta) = d_o e^{-\xi(r,\theta)}[1 - n \cdot \xi(r,\theta)] \quad (9)$$

where

$$\xi(r,\theta) = k \cdot \left(\frac{\pi}{c}\right)^n \cdot (\sin^2\theta + c^2 \cos^2\theta) \cdot r^{2n} \quad (10)$$

Regional Storm Characteristics and Distributional Assumptions

The aforementioned simplified description of the storm's spatial pattern results in the representation of the random vector Λ_s by the following random variables

$$\Lambda_s = (D_o\ K\ N\ C\ \Phi)' \quad (11)$$

where $'$ denotes transpose, and D_o, K, N, C, and Φ denote the random variables taking on values d_o, k, n, c, and ϕ, respectively. Thus, for estimation of the joint probability distribution $f_{\Lambda_s\Lambda_p}(\boldsymbol{\lambda}_s, \boldsymbol{\lambda}_p)$ needed in Eq. 3*b* one needs to estimate the joint probability distribution $f_{\Omega}(\boldsymbol{\omega})$ where

$$\boldsymbol{\Omega} = (D_o\ K\ N\ C\ \Phi\ X\ Y)' \quad (12)$$

and (X,Y) denotes the random vector of the spatial coordinates of the storm-center position. Then, Eq. 4 becomes

$$G(d) = 1 - \int_{\Omega} \text{pr}[d_c(\Delta t) \le d|\boldsymbol{\omega}] f_{\Omega}(\boldsymbol{\omega}) d\boldsymbol{\omega} \quad (13)$$

From a statistical and cross-correlational analysis of the characteristics of the analyzed storms, the following properties were revealed and used for the estimation of the joint probability distribution $f_{\Omega}(\boldsymbol{\omega})$:

1. The storm orientation Φ is independent of all other random variables of the vector $\boldsymbol{\Omega}$. In the present implementation, the estimation of the marginal distribution $f_{\Phi}(\phi)$ was not considered, due to the lack of maximum 24-hour storm-orientation data. Thus, the estimation of $G(d)$ was restricted to circular catchments for which the storm orientation ϕ will have no effect on the estimate of $G(d)$ and the integration over the parameter Φ need not be considered.
2. The storm elongation parameter C is independent of all other random variables of the vector $\boldsymbol{\Omega}$ and follows a distribution $f_C(c)$. To simplify the estimation of $G(d)$, however, this parameter was taken to be as a constant ($c = 2.0$). As can be seen from Fig. 2, a large percentage of the extreme storms from the catalog have a total depth-shape parameter of 2.0, or a value of 1.5 or 2.5. In Foufoula-Georgiou (1989a), it was shown that a difference of ± 0.5 in the specification of the parameter c of a storm had little effect on the estimation of the exceedance probabilities. (This finding was confirmed by a more extensive sensitivity analysis as will be reported in a later section.) Thus, it was assumed that fixing C to 2 and not integrating over its distribution would have little effect on the estimation of $G(d)$.

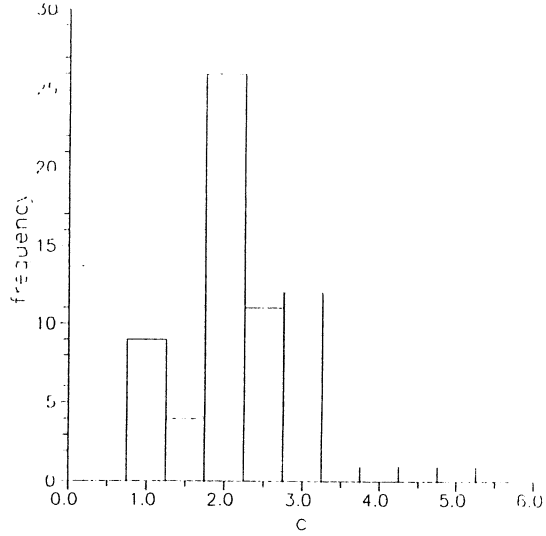

FIG. 2. Empirical Distribution of Parameter c

3. The parameters K and N of the spatial spread function of Eq. 8 are dependent upon each other but independent of all other random variables of the vector $\boldsymbol{\Omega}$. If we let $K' = \ln K$, then the pair (K',N) follows a bivariate normal distribution

$$f_{K'N}(k',n) = \frac{1}{2\pi\sigma_{K'}\sigma_N\sqrt{1-\rho^2}} \cdot \exp\left[-\frac{1}{2}Q(K',N)\right] \quad (14)$$

where

$$Q(K',N) = \frac{1}{1-\rho^2}\left[\left(\frac{k'-\mu_{K'}}{\sigma_{K'}}\right)^2 - 2\rho\left(\frac{k'-\mu_{K'}}{\sigma_{K'}}\right)\left(\frac{n-\mu_N}{\sigma_N}\right) + \left(\frac{n-\mu_N}{\sigma_N}\right)^2\right] \quad (15)$$

Empirical frequency distributions of the parameters k' and n are given in Figs. 3(*a*) and 3(*b*), respectively. Estimates of these parameters were obtained by a weighted least-squares fit of Eq. 8 to the maximum 24-hour depth-area data for storm areas of 10–10,000 sq mi. For larger storms, where the storm area enclosed within the contour of 3 in. was greater than 10,000 sq mi, the areas beyond 10,000 sq mi were also included in the fit. Then, estimates of the parameters $(\mu_{K'}, \sigma_{K'}, \mu_N, \sigma_N, \rho_{K'N})$ of the bivariate normal distribution were ob-

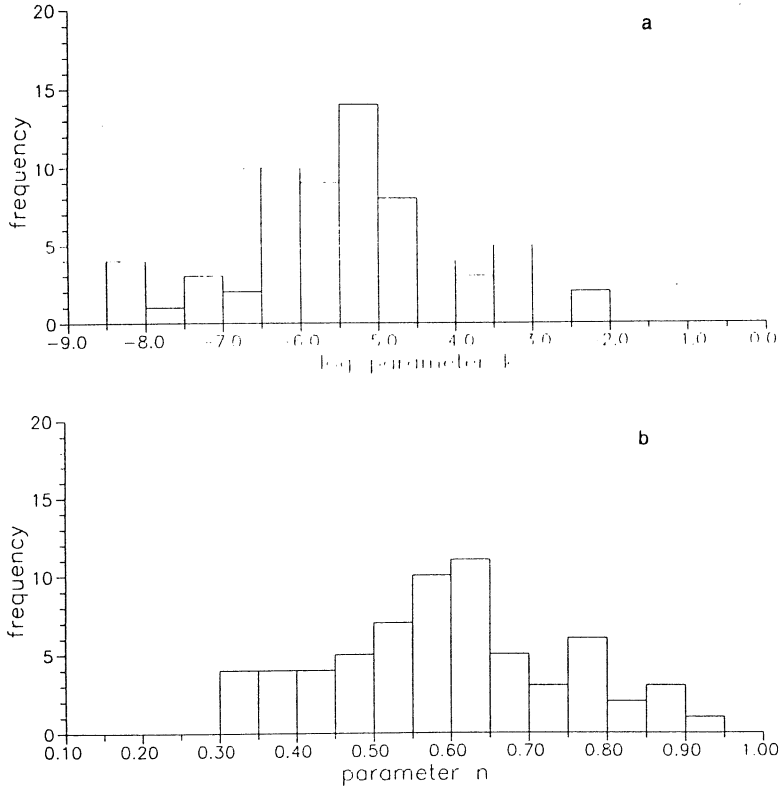

FIG. 3. (*a*) Empirical Distribution of Parameter $k' = \ln k$; (*b*) Empirical Distribution of Parameter n

tained as: $\hat{\mu}_{K'} = -5.437$, $\hat{\sigma}_{K'} = 1.335$; $\hat{\mu}_N = 0.597$, $\hat{\sigma}_N = 0.147$; and $\hat{\rho} = \hat{\rho}_{K'N} = -0.917$.

4. The coordinates of the random location (X, Y) of the storm center are independent of all other random variables of Ω except D_o, the maximum 24-hour storm-center depth. The joint probability distribution $f_{XYD_o}(x, y, d_o)$ is estimated by first characterizing the conditional probability density function (pdf) $f_{XY|D_o}(x, y|d_o)$ and then the marginal pdf $f_{D_o}(d_o)$. Based on empirical evidence and a statistical analysis of the spatial position of storm centers within the major nine-state area A_{tr}, it is hypothesized that different distributions $f_{XY|D_o}(x, y|d_o)$ hold for storm-center depths $d_o < d_{\min}$ and $d_o \geq d_{\min}$, where $d_{\min}$ is a prespecified cutoff depth. For $d_o < d_{\min}$—that is, for less extreme storms—the distribution of the storm centers is assumed to be homogeneous. Then, the probability density function for the random vector (X, Y) is uniform and given by

$$f^{(1)}_{XY}(x, y) \equiv f_{XY|D_o<d_{\min}}(x, y|d_o < d_{\min}) = \frac{1}{|A_{tr}|} \cdot I(x, y) \quad \ldots\ldots (16)$$

where $I(x, y)$ is an indicator function defined over the region A_{tr} as

$$I(x, y) = 1 \qquad \text{if } (x, y) \in A_{tr} \quad \ldots\ldots (17a)$$

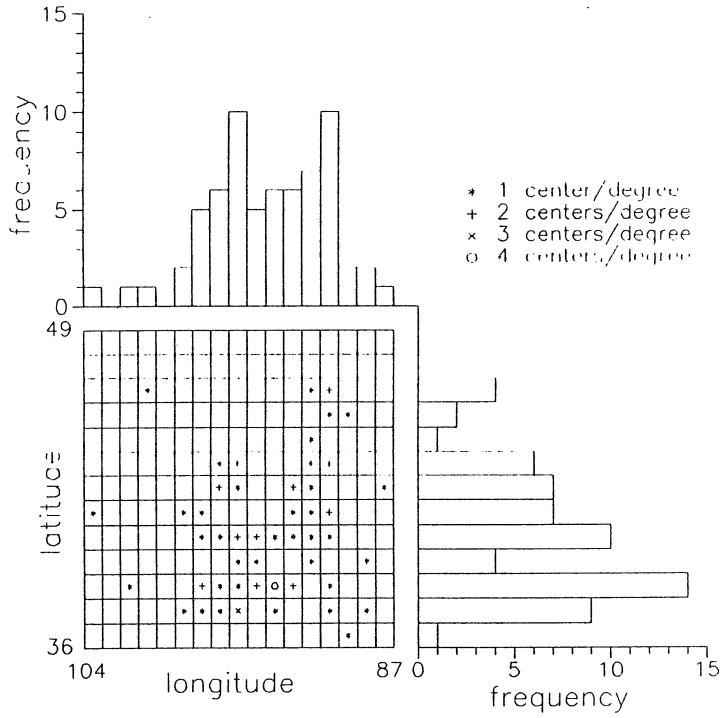

FIG. 4. Spatial Occurrence of Storm Centers as Function of Latitude and Longitude

$$I(x, y) = 0 \qquad \text{otherwise} \quad \ldots\ldots (17b)$$

For $d_o \geq d_{\min}$, there is strong evidence that extreme storms have preferred storm-center locations, with a larger probability of occurrence in the south and southeast and smaller probability of occurrence in the north and northwest region of the transposition area A_{tr}. Thus, the spatial distribution of storm centers is, in general, characterized by a nonhomogeneous anisotropic point process within the area A_{tr}. Based on observations related to the spatial distribution of extreme rainfall depths in the Midwest [see Fig. 4 reproduced from Foufoula-Georgiou and Wilson (1990)], it was hypothesized that the distribution of (X, Y) conditional on $d_o \geq d_{\min}$ (where $d_{\min}$ remains to be specified) could be represented as a transformed bivariate normal distribution independent in each direction. Thus

$$f^{(2)}_{XY}(x, y) \equiv f_{XY|D_o \geq d_{\min}}(x, y|d_o \geq d_{\min}) = f^{(2)}_X(x) \cdot f^{(2)}_Y(y) \quad \ldots\ldots (18)$$

where

$$f^{(2)}_X(x) = \frac{1}{\sqrt{2\pi}\,\sigma_X} \cdot \exp\left[-\frac{1}{2}\left(\frac{x - \mu_X}{\sigma_X}\right)^2\right], \qquad -\infty < x < \infty \quad \ldots\ldots (19)$$

and

FIG. 5. Coordinate System for Distribution $f_{XY}^{(2)}(x,y)$ and Locations of 16 Catchments within Nine-State Region

$$f_Y^2(y) = \frac{\sqrt{2}}{\sqrt{\pi}\,\sigma_o} \cdot \exp\left\{-\frac{1}{2}\left(\frac{y-\mu_o}{\sigma_o}\right)^2\right\} \quad \text{for } \mu_o \le y < \infty \quad \ldots\ldots (20a)$$

$$f_Y^2(y) = 0 \quad \text{for } -\infty < y < \mu_o \quad \ldots\ldots (20b)$$

In the previous equations, all distances are with respect to a global coordinate system positioned arbitrarily at the point of latitude 35° N and longitude 105° W outside the nine-station region shown in Fig. 5. The parameters $(\mu_X, \sigma_X, \mu_o, \sigma_o)$ of the model remain to be estimated from the data, as will be discussed in this section. Note that $f_{XY}^{(2)}(x,y)$ is a probability density function on the upper half-plane of a local coordinate system centered at point $O = (\mu_X, \mu_o)$ (see Fig. 5) and thus it satisfies

$$\int_{\mu_o}^{\infty}\int_{-\infty}^{\infty} f_{XY}^{(2)}(x,y)\,dy\,dx = 1$$

Combining the two distributions, one obtains

$$f_{XYD_o}(x,y,d_o) = f_{XY}^{(1)}(x,y) \cdot F_{D_o}(d_{\min}) + f_{XY}^{(2)}(x,y) \cdot [1 - F_{D_o}(d_{\min})] \quad \ldots\ldots (21)$$

where $F_{D_o}(d_{\min}) = \text{pr}(d_o < d_{\min})$ refers to the cumulative distribution function of D_o. Empirical evidence suggests that the cutoff level $d_{\min}$ (for homogeneous versus nonhomogeneous distribution of storm centers) is less than 8 in. Thus, since the set of extreme storms used in this study includes only storms for which the maximum 24-hour depth d_o is greater than or equal to 8 in., Eq. 21 reduces to:

$$f_{XYD_o}(x,y,d_o) = f_{XY}^{(2)}(x,y) \cdot [1 - F_{D_o}(d_{\min})] \quad \ldots\ldots (22)$$

where $f_{XY}^{(2)}(x,y)$ is given by Eq. 18. The parameters $(\mu_X, \sigma_X, \mu_o, \sigma_o)$ of the transformed bivariate normal distribution were estimated as follows. From Eq. 19 it is obvious that μ_X can be estimated as the mean horizontal distance of all storm-center positions with respect to the global coordinate system, and σ_X as the standard deviation of these distances. These estimates were $\hat{\mu}_X = 589$ mi and $\hat{\sigma}_X = 150$ mi. From Eq. 20 one can derive the following relationships between the first two moments of the random variable Y (vertical distance of the storm center positions with respect to the global coordinate system) and the parameters μ_o and σ_o of the distribution $f_Y^{(2)}(y)$

$$\mu_Y = \mu_o + \frac{2\sigma_o}{\sqrt{2\pi}} \quad \ldots\ldots (23)$$

$$\sigma_Y = \sigma_o \sqrt{\frac{\pi - 2}{\pi}} \quad \ldots\ldots (24)$$

Based on these relationships and the estimates of $\hat{\mu}_Y = 398$ mi and $\hat{\sigma}_Y = 179$ mi obtained from the data, it was found that $\hat{\mu}_o = 161$ mi and $\hat{\sigma}_o = 297$ mi. Note that with these estimates, the south boundary of the Midwest area is determined by the $\hat{\mu}_o = 161$ mi horizontal line, and the other three geographical boundaries of the Midwest area are fairly well approximated by the distances $\pm 3\hat{\sigma}_X$ (east, west) and $3\hat{\sigma}_o$ (north) according to the model $f_{XY}^{(2)}(x,y)$.

5. The frequency distribution of the maximum 24-hour storm-center depth D_o (see Fig. 6) was modeled by a shifted exponential distribution given by

$$f_{D_o}(d_o) = \frac{1}{\theta} \exp\left[-\frac{(d_o - d_{\min})}{\theta}\right] \quad \ldots\ldots (25)$$

with $d_{\min} = 8.0$ as previously discussed. The parameter θ was estimated as $\hat{\theta} = 2.38$ in.

6. The number of extreme storm occurrences per year (see Fig. 7) was modeled by a Poisson distribution given by

$$\text{pr}[Z(1) = \nu] = \frac{e^{-\lambda}\lambda^{\nu}}{\nu!}, \qquad \nu = 0, 1, 2, \ldots \quad \ldots\ldots (26)$$

The parameter λ, which is equal to the mean number of storms per year, was estimated as 1.07 storms/year.

Estimation of Exceedance Probability $G(d)$

Based on the aforementioned postulates regarding the joint probability distribution of the random vector Ω, Eq. 13 can be written as

$$G(d) = 1 - \int_{D_o}\int_{Y}\int_{X}\int_{N}\int_{K'}\int_{C}\int_{\Phi} \text{pr}[\bar{d}_e(\Delta t)$$

$$\le d|\phi, c, k', n, x, y, d_o]\,dF_{\Phi}(\phi)\,dF_C(c)\,dF_{K'N}(k', n)\,dF_{XYD_o}(x,y,d_o) \quad \ldots\ldots (27)$$

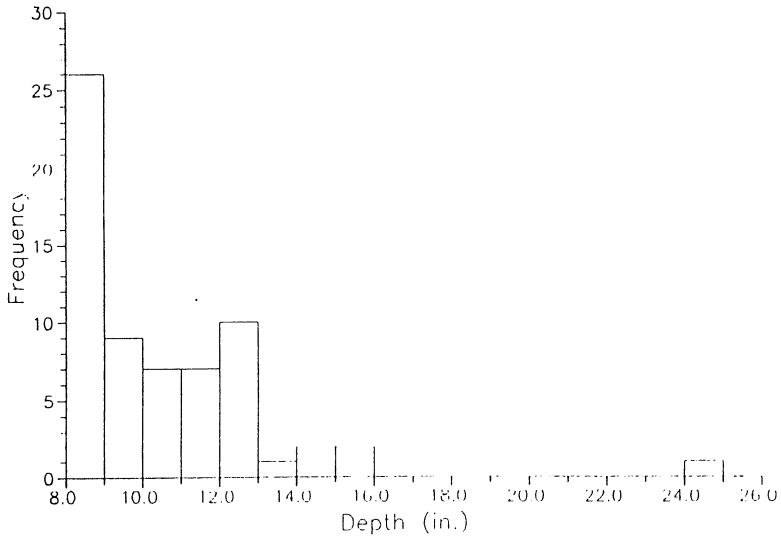

FIG. 6. Empirical Distribution of Parameter d_o

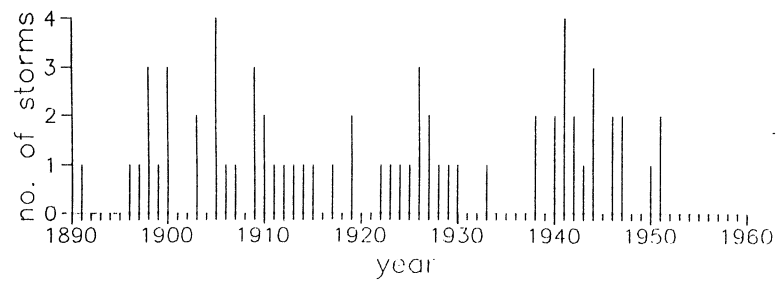

FIG. 7. Distribution of Number of Storms per Year

which, based on the results from the previous section, can now be written as

$$G(d) = 1 - \int_{D_o}\int_{Y}\int_{X}\int_{N}\int_{K'} \mathrm{pr}[\bar{d}_c(\Delta t) \le d|k', n, x, y, d_o] f_{K'N}(k', n) f^{(2)}_{XY}(x, y) f_{D_o}(d_o) dk'dn\, dx\, dy\, dd_o \quad (28)$$

Estimation of $G(d)$ is performed as follows. Synthetic storms are generated with elliptical shape of major-to-minor axis equal to 2, storm center depth equal to d_o [sampled from $f_{D_o}(d_o)$], and spatial distribution described by the spread function of Eq. 8 with parameters (k', n) [sampled from $f_{K'N}(k', n)$]. Due to the randomness of (d_o, k', n) the areal extent of the storm (defined as the area enclosed within the contour depth of 3 in.) is also random. These storms are positioned within the storm transposition area A_{tr} according to the spatial occurrence distribution model $f^{(2)}_{XY}(x, y)$ of their centers. Since not all storms centered within the transposition area A_{tr} will contribute a nonzero depth $\bar{d}_c(\Delta t)$ to the catchment, the simulation is simplified by transposing storms only within the effective area of the catchment. The effective area (A_{eff}) is defined as the area within which a storm, if it is centered, will have at least one point common with the catchment. Although in general, A_{eff} can be defined by the Minkowski addition of the catchment and storm areas

$$A_{eff} = A_c \oplus A_s \quad (29)$$

(Serra 1982), its geometrical shape cannot be easily described parametrically. Instead, it must be determined numerically, except for special cases, as for example a circular storm (of radius r_s) and circular catchment (of radius r_c) where A_{eff} is also circular (with radius $r_c + r_s$). Note that A_{eff} changes every time a new storm is transposed over the catchment of interest.

To simplify the estimation it is assumed that the storm centers follow a uniform distribution within A_{eff}—that is, the probability of a storm center occurring at any point within A_{eff} is constant and equal to $\mathrm{pr}[(x, y) \in A_{eff}]$, which is evaluated from the integration of $f^{(2)}_{XY}(x, y)$ over A_{eff}. This assumption improves the computational efficiency of the estimation and is not critical since A_{eff} is very small compared to the whole transposition area A_{tr}. In view of this, Eq. 28 may now be written as

$$G(d) = 1 - \int_{D_o = d_{\min}}^{\infty} f_{D_o}(d_o) \int_{K' = -\infty}^{\infty} \int_{N=0}^{\infty} \{1 - \mathrm{pr}[\bar{d}_c(\Delta t) \ge d|k', n, d_o, (x, y) \in A_{eff}]\} \mathrm{pr}[(x, y) \in A_{eff}] f_{K'N}(k', n) dk'dn\, dd_o \quad (30)$$

By sampling (k', n, d_o) triplets from their respective distributions, using these triplets to construct storms and transposing the storms at grid points within A_{eff}, the integration is evaluated numerically. The terms to be estimated are

$$I_1 = \mathrm{pr}[\bar{d}_c(\Delta t) \ge d|k', n, d_o, (x, y) \in A_{eff}] \quad (31)$$

and

$$I_2 = \mathrm{pr}[(x, y) \in A_{eff}] = \int\int_{A_{eff}} f^{(2)}_{XY}(x, y) dx dy \quad (32)$$

If $\bar{d}_{c_j}$ = the average depth over the catchment from a storm with given parameters (k', n, d_o) and centered at position $(x, y)_j$, I_1 is estimated as

$$\hat{I}_1 = \frac{1}{N} \sum_{j=1}^{N} I(\bar{d}_{c_j} \ge d) \quad (33)$$

where

$$I(\bar{d}_{c_j} \ge d) = 1 \quad \text{if } \bar{d}_{c_j} \ge d \quad (34a)$$

$$I(\bar{d}_{c_j} \ge d) = 0 \quad \text{otherwise} \quad (34b)$$

and N = the total number of sampled storm-center positions within A_{eff}. The second probability, I_2, can be evaluated by numerical integration of $f^{(2)}_{XY}(x, y)$ over the effective area. For computational efficiency this integral can also be evaluated semianalytically after a small approximation is introduced, as described in Appendix I.

Results of Implementation

As previously stated, the transposition area A_{tr} consists of a nine-state region in the Midwest. To capture the variability of the exceedance probability estimates within the Midwest, 16 sites were selected in A_{tr}, each site having

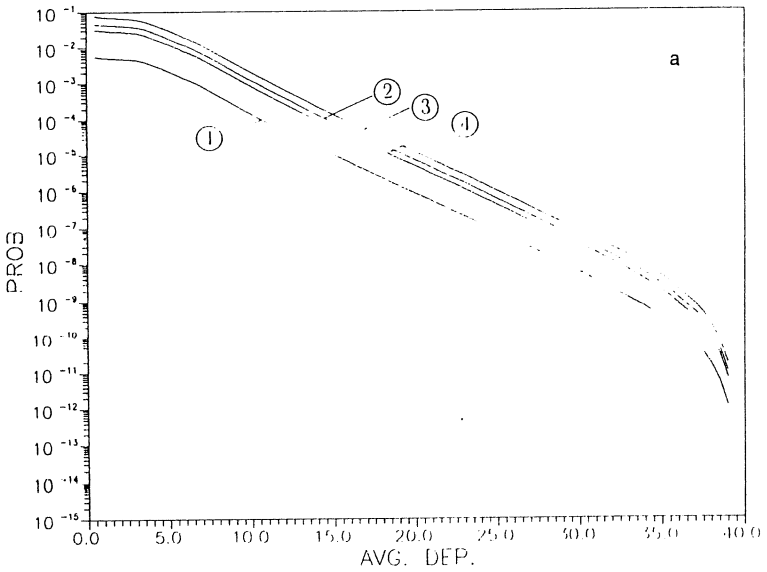

FIG. 8. (*a*) Annual Exceedance Probability $G^a(d)$ for Catchments One–Four

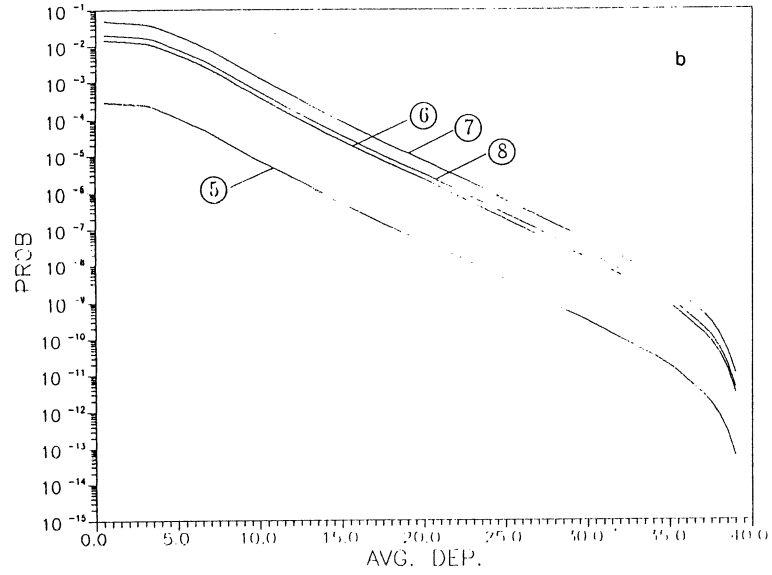

FIG. 8. (*b*) Annual Exceedance Probability $G^a(d)$ for Catchments Five–Eight

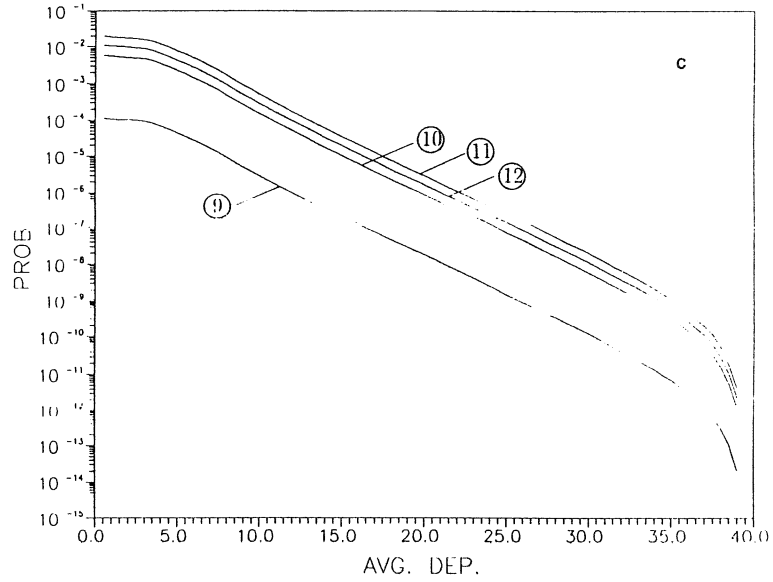

FIG. 8. (*c*) Annual Exceedance Probability $G^a(d)$ for Catchments Nine–12

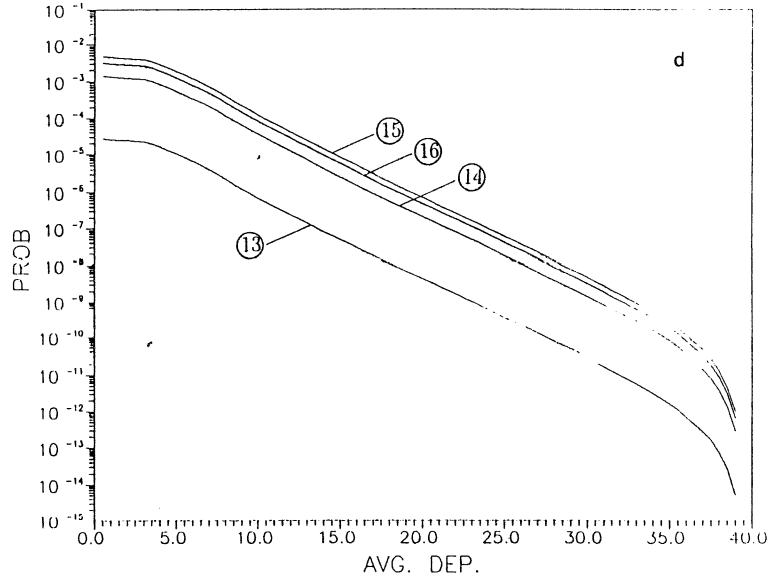

FIG. 8. (*d*) Annual Exceedance Probability $G^a(d)$ for Catchments 13–16

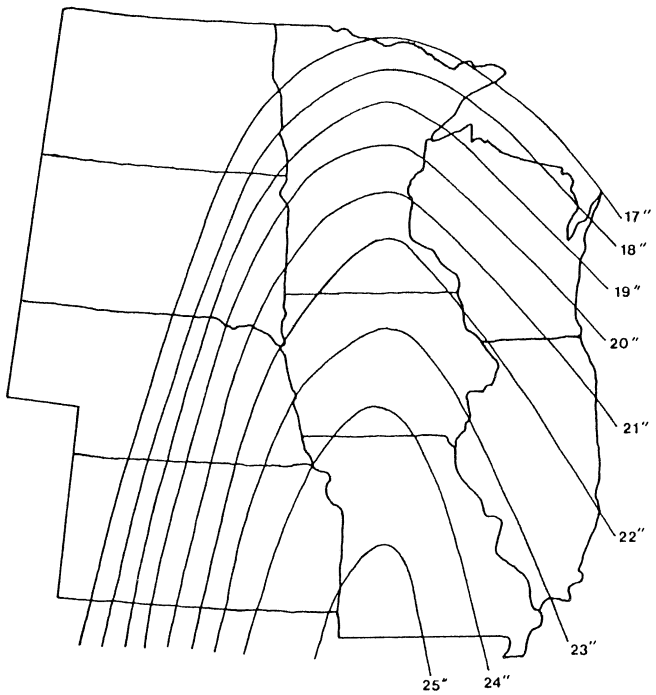

FIG. 9. Contours for 10^{-6} Event (24-hour 100 sq mi Average Depth)

a circular catchment with an area of 100 sq mi. The locations of the centers of these catchments are given in Fig. 5. The regional variation in the annual exceedance probability estimates $G^a(d)$ will be solely due to the nonhomogeneous distribution of the storm-center locations.

Figs. 8(*a*)–8(*d*) give the estimated curves for $G^a(d)$ for all 16 catchments. Using the information from these curves, contour maps of the 24-hour average rainfall depths deposited over 100-sq mi catchments and having specified exceedance probabilities, e.g., 10^{-3}, 10^{-6}, or 10^{-9}, can be constructed. For example, the map of the 10^{-6} event is shown in Fig. 9.

This figure shows that, in general, the trend of the spatial variability of extreme precipitation depths in the Midwest is captured [compare, for example, Fig. 9 with figures of PMP estimates in Hershfield (1961)]. The gradient in the western (and to a lesser degree in the eastern) part of the region, however, is much steeper than that expected from meterological considerations. These steep gradients are of course the result of the assumed transformed bivariate normal distribution for the storm-center positions, which for the estimated parameters assumes almost zero probability of storm occurrences at the west and east boundaries of the studied region. Milder gradients can be obtained by adjusting the parameters of this distribution to acknowledge that such storms can occur outside the area of interest with nonzero probability. Such refinements and the possibility of directly incorporating meteorological information into the estimation procedure of the storm-center distribution are presently under study.

Although the estimates given in the present paper are still preliminary and should not be used for design purposes, they clearly demonstrate the ability of the stochastic storm transposition methodology to provide an objective means of arriving at realistic, comparatively consistent regional estimates of storm exceedance probabilities. Moreover, the method provides a vehicle for performing objective comparative risk studies within a region or among regions in a more constructive way than using, for example, the limited relative conservatism index proposed by Wang and Revell (1983). Comparative risk studies are very helpful in resource allocation decisions arising from retrofitting evaluation of existing structures declared inadequate under the current PMP/PMF design criteria [e.g., Dawdy and Lettenmaier (1987)]. An additional important aspect of the SST method is that it provides the means of performing uncertainty analysis of the estimates that can be incorporated in the risk-based decision-making methodology. Some preliminary sensitivity analysis results are presented in the next section.

Sensitivity Analysis

A preliminary sensitivity analysis was performed to test the robustness of the estimates to uncertainties in the data and uncertainties in the estimation procedure itself. Uncertainties in the data may come from the underestimation of recorded storm depths [e.g., Foufoula-Georgiou (1989b)] and the omission of storms from the catalog. Uncertainties in the procedure may come from the difficulty in estimating the parameters from small samples as well as from several assumptions introduced for simplicity or lack of data, as, for example, the assumption of fixed-storm ellipticity or the assumption of single-center storms versus more realistic complex spatial patterns.

Case 1

To assess the effect of an incomplete catalog on the estimates, an omission rate of 20% was assumed for all storms, based on their rate of occurrence. Assuming that all the other properties of the storms remain unchanged (which might not be true in reality), only the parameter λ was changed. Initially estimated as 1.07, it was reestimated as $\lambda' = 1.28$ storms/year. In effect, this means 78 storms with storm-center depth exceeding 8 in. actually occurred during the period of record, but only 65 were documented in the storm catalog. The estimated curves for $G^a(d)$ (not reproduced here due to space limitations) did not show any appreciable differences from the original ones. This is to be expected when one examines Eq. 6 for the λ values used for the two cases.

Case 2

A more realistic case of assessing the effects of an incomplete storm catalog was also performed. This involved dividing the storm set into two groups with different omission rates. This would seem a more reasonable model of storm omission since the most severe storms would have a much smaller chance of being omitted from the storm catalog compared to the less severe storms. The two omission rates were specified as $8 \leq d_o < 10$ in. = 30% and $d_o \geq 10$ in. = 5%. This enlarged the original set from 65 to 81 storms. Now, both the distribution of storm-center depths, $f_{D_o}(d_o)$, and the distribution of storm occurrences per year, $\text{pr}[Z(1) = \nu]$, changed. The new parameters were estimated as $\hat{\theta}'' = 2.04$ in. and $\hat{\lambda}'' = 1.33$ storms/year. For this case, the differences in the estimates of $G^a(d)$ were more appreciable,

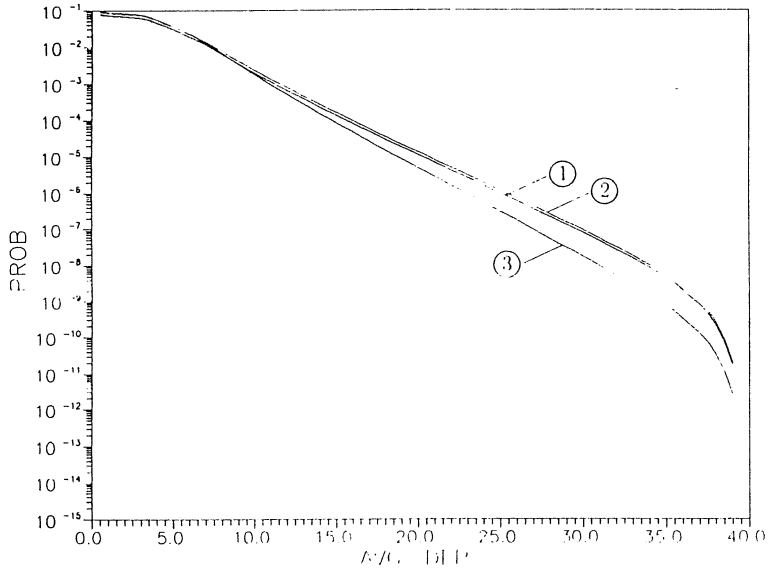

FIG. 10. Comparison of Annual Exceedance Probability $G^a(d)$ for Catchment 3: (1) Original Data; (2) Case of Uniform Omission Rate; and (3) Case of Nonuniform Omission Rate

but still within an order of magnitude from the original estimates, despite the assumed high omission rate. For comparison purposes, the estimated curves for the original data and the two cases just presented, are shown here for area three in Fig. 10. It is observed for example, that for a 100-sq mi catchment in central Missouri, the 24-hour average depth of 30 in. would have an annual exceedance probability of 10^{-7} (original and case 1) and approximately 10^{-8} (case 2). In our opinion, this is an encouraging result given that the assumed omission rate of 30% is higher than that expected in reality.

Case Three

To assess the effect of the variation in the storm shape parameter c, which was assumed to be equal to its most likely value of 2.0, the estimation was reevaluated assuming c to be equal to 2.5 and 3.0. For the 100-sq mi catchment area used herein, the effect of this variation on the estimates of $G^a(d)$ was unnoticeable and the curves were not presented here.

Sensitivity analysis of the estimates to underestimation of storm depths and assumptions regarding the spatial distribution of depths within the storm are currently under investigation and the results will be reported in the future.

Summary and Concluding Remarks

In an earlier study, Foufoula-Georgiou (1989a) presented the general methodology and estimation problems associated with the stochastic storm

transposition (SST) approach for the estimation of exceedance probabilities of extreme precipitation depths. This method has been further advanced and refined in this paper, and implemented for the Midwest.

Under the assumptions of an elliptical storm shape and spread function of a given functional form, extreme storms have been described by the joint probability distribution of seven storm parameters (five specifying the magnitude, orientation, shape, and within-storm spatial variability, and two specifying the location of the storm center). A nonhomogeneous spatial multivariate point process model has been postulated for the joint probability distribution of the storm-center depth and storm location and it has been fitted to 65 extreme storms in the nine-state Midwestern region. The method has been used to estimate the tails of the probability distribution of the average catchment depths over several hypothetical catchments in the Midwest and describe the spatial variability of the estimates over the studied region. The results of a preliminary sensitivity analysis are encouraging in that the method shows robustness to some of the uncertainties (e.g., storm catalog incompleteness) that are of concern to most hydrologists. It should be kept in mind that, from the practical standpoint, one only need estimate the exceedance probabilities with an accuracy that falls within the range of probabilities that would not significantly affect the design or decision-making process.

Although further refinements of the method are needed, mainly related to the distributional assumption of storm-center positions that directly affects the regional variability of the estimates, the potential of the method to provide an objective basis for extreme storm probability assessment has been demonstrated. Such refinements are currently under investigation in parallel with a more extensive sensitivity analysis of the estimates to several distributional assumptions and uncertainties inherent in the data and estimation procedures.

As a final remark, we want to briefly elaborate on a very important issue that lies at the heart of any extreme event analysis, but is often misinterpreted. Several investigators are skeptical of methods attempting to estimate events of low annual frequency, i.e., less than 10^{-3}. The major criticism is the lack of stationarity of climate and precipitation over periods of thousands of years. This criticism is unfounded and arises from the misconception that the event of annual exceedance probability, e.g., 10^{-5}, should be equivalently interpreted as an event that will be exceeded on the average only once in a 100,000 years. But who really knows what the state of this planet will be in a 100,000 years, leaving aside that no hydraulic structure of today will be in place to witness failure or success from that once-in-a-1,000,000-years flood! It should be made clear that the assumption of stationarity over millions of years is neither made nor implied in rare event probability assessment studies as the one presented herein. Rather, the assumption of stationarity is made only over the period of record used in the analysis (61 years in this study) and this is not even necessary as evidence to the contrary should be incorporated in the methodology. Thus, the rainfall event with 10^{-5} annual exceedance probability should be interpreted as the event that has a probability of exceedance in the next year (and any subsequent year if no other changes are identified) equal to 10^{-5}. These probabilities should be revised as new data or new information about climate change become available. We hope this clarification will help resolve this unfortunate misconception that seems to have hindered progress on extreme event analysis.

Acknowledgments

This material is based upon work supported by the National Science Foundation under grants CES-8708825 and BSC-8957469. This support is gratefully acknowledged.

Appendix I. Estimation of I_2

The integral to be evaluated is

$$I_2 = \int\int_{A_{eff}} f_{XY}^{(2)}(x,y)dxdy \quad (35)$$

where $f_{XY}^{(2)}(x,y)$ is given in Eq. 18. Throughout the appendix we simplify $f_{XY}^{(2)}(x,y)$ to $f(x,y)$, which, due to the independence assumption, may be written as $f(x)\cdot f(y)$. To simplify the numerical evaluation of this integral, the assumption is made that the effective area is elliptical. This is not a bad approximation given that we deal with a circular catchment that is small with respect to the size of the elliptical storm. For the ellipse representing the effective area, let (c,d) denote the coordinates of its center with respect to the global coordinate system (x,y), and a and b denote the major and minor axes. The lengths a and b are equal to $(r_c + r_1)$ and $(r_c + r_2)$, where r_c = the radius of the circular catchment and r_1 and r_2 = the major and minor axes of the ellipse representing the storm. Using the equation of the ellipse

$$\frac{(x-c)^2}{a^2} + \frac{(y-d)^2}{b^2} = 1 \quad (36)$$

one obtains

$$y = d \pm b\cdot\sqrt{1 - \frac{(x-c)^2}{a^2}} \quad (37)$$

The integration of the surface $f(x,y) = f(x)\cdot f(y)$ over the ellipse gives

$$I_2 = \oint f(x,y)dxdy = \int_{c-a}^{c+a} f(x)h(x)dx \quad (38)$$

where

$$h(x) = \int_{d-b\sqrt{1-[(x-c)^2/a^2]}}^{d+b\sqrt{1-[(x-c)^2/a^2]}} f(y)dy \quad (39)$$

Introducing $f(y)$ in the previous integral, results in

$$h(x) = \text{erf}\left(\frac{\frac{b}{a}\sqrt{a^2-(x-c)^2} + \mu_u - d}{\sqrt{2}\sigma_u}\right) + \text{erf}\left(\frac{\frac{b}{a}\sqrt{a^2-(x-c)^2} - \mu_u + d}{\sqrt{2}\sigma_u}\right) \quad (40)$$

where erf $(\cdot)$ denotes the error function given by (Abramowitz and Stegun 1972)

$$\text{erf } z = \frac{2}{\sqrt{\pi}}\int_0^z e^{-t^2}dt \quad (41)$$

The integral I_2 is then evaluated from Eq. 38 by numerical integration on a line, not on a surface.

Appendix II. References

Abramowitz, M., and Stegun, I. A. (1972). *Handbook of mathematical functions*. Dover Publications, Inc., New York, N.Y.

Alexander, G. N. (1963). "Using the probability of storm transposition for estimating the frequency of rare floods." *J. Hydrol.*, 1(1), 46–57.

Buehler, B. (1984). Discussion of "realistic assessment of maximum flood potentials," by D. W. Newton. *J. Hydr. Engrg.*, ASCE, 110(8), 1166–1168.

Dawdy, D. R., and Lettenmaier, D. P. (1987). "An initiative for risk-based flood design." *J. Hydr. Engrg.*, ASCE, 113(8), 1041–1051.

Fontaine, T. A., and Potter, K. W. (1989). "Estimating probabilities of extreme rainfalls." *J. Hydr. Engrg.*, ASCE, 115(11), 1562–1575.

Foufoula-Georgiou, E. (1989a). "A probabilistic storm transposition approach for estimating exceedance probabilities of extreme precipitation depths." *Water Resour. Res.*, 25(5), 799–815.

Foufoula-Georgiou, E. (1989b). "On the accuracy of the maximum recorded depth in extreme rainstorms." *Proc. IAHS Third Scientific Assembly*, International Association of Hydrological Sciences, 181, 41–49.

Foufoula-Georgiou, E., and Wilson, L. L. (1990). "In search of regularities in extreme rainstorms." *J. Geophys. Res.*

Gupta, V. K. (1972). "Transposition of storms for estimating flood probability distributions." *Hydrology Paper 59*, Colorado State Univ., Fort Collins, Colo.

Hershfield, D. M. (1961). "Rainfall frequency atlas of the United States for durations from 30 minutes to 24 hours and return periods from 1 to 100 years." *Weather Bureau Tech. Paper No. 40*, U.S. Dept. of Commerce, Washington, D.C., 93–105.

Myers, V. A. (1967). "Meteorological estimation of extreme precipitation for spillway design floods." *Weather Bureau Tech. Memo WBTM-HYDRO-5*, U.S. Dept. of Commerce, Silver Spring, Md., 1–28.

Newton, D. W. (1983). "Realistic assessment of maximum flood potentials." *J. Hydr. Engrg.*, ASCE, 109(6), 905–918.

Serra, J. (1982). *Image analysis and mathematical morphology*. Academic Press, London, United Kingdom, 43.

Stedinger, J., and Grygier, J. (1985). "Risk-cost analysis and spillway design." *Computer applications in water resources*, H. C. Torno, ed., ASCE, New York, N.Y., 1208–1217.

Storm rainfall in the United States. (1945–1990). Office of the Chief of Engineers, U.S. Army Corps of Engineers, Washington, D.C.

Wang, B. H. (1984). "Estimation of probable maximum precipitation: Case studies," *J. Hydr. Engrg.*, ASCE, 110(10), 1457–1472.

Wang, B. H., and Revell, R. W. (1983). "Conservatism of probable maximum flood estimates." *J. Hydr. Engrg.*, ASCE, 109(3), 400–408.

Appendix III. Notation

The following symbols are used in this paper:

A_c = catchment area;
A_{eff} = storm effective area;
A_s = storm area;
A_{tr} = storm transposition area;
c = major to minor axis of storm elliptical shape;
$d(r,\theta)$ = rainfall depth at distance r from storm center and angle θ from storm orientation axis;

$d(x,y,t)$ = rainfall depth at point of spatial coordinates (x,y) during time period $(0,t]$;
$d_{\min}$ = specified cutoff rainfall depth;
d_o = maximum 24-hour recorded depth (taken as storm center depth);
$\bar{d}(A)$ = maximum 24-hour average depth over area A;
$\bar{d}_c(\Delta t)$ = maximum average depth over catchment area A_c during time period Δt;
$erf\ z$ = error function of z;
$F_{\bar{d}_c(\Delta t)}(d)$ = $F(d)$ = cumulative distribution function of $\bar{d}_c(\Delta t)$;
$F^a_{\bar{d}_c(\Delta t)}(d)$ = $F^a(d)$ = annual nonexceedance probability of $\bar{d}_c(\Delta t)$;
$F_{\Lambda_s\Lambda_p}(\boldsymbol{\lambda}_s,\boldsymbol{\lambda}_p)$ = cumulative joint distribution function of random vectors Λ_s and Λ_p;
$f_{D_o}(d_o)$ = probability density function of the storm-center depth D_o;
$f^{(1)}_{XY}(x,y)$ = probability density function of the random vector (X,Y) for $D_o < d_{\min}$;
$f^{(2)}_{XY}(x,y)$ = probability density function of the random vector (X,Y) for $D_o \geq d_{\min}$;
$f_{\Lambda_s\Lambda_p}(\boldsymbol{\lambda}_s,\boldsymbol{\lambda}_p)$ = joint probability distribution of the random vectors Λ_s and Λ_p;
$f_{\Omega}(\boldsymbol{\omega})$ = probability density function of the random vector Ω;
$G_{\bar{d}_c(\Delta t)}(d)$ = $G(d)$ = exceedance probability of $\bar{d}_c(\Delta t)$;
$G^a_{\bar{d}_c(\Delta t)}(d)$ = $G^a(d)$ = annual exceedance probability of $\bar{d}_c(\Delta t)$;
$I(x,y)$ = indicator function defined in Eq. 17;
$I(\bar{d}_{c_j} \geq d)$ = indicator function defined in Eq. 34;
I_1 = function defined in Eq. 31;
I_2 = function defined in Eq. 32;
k,n = parameters of the average depth-area relationship;
k' = $\ln k$;
t_r = storm duration;
$Z(t)$ = number of extreme storms in interval of t years;
Λ_p = random vector of storm-center location;
Λ_s = random vector of storm characteristics;
$\mu_{K'},\sigma_{K'}$ = mean and standard deviation of parameter K';
μ_N,σ_N = mean and standard deviation of parameter N;
$\mu_X,\sigma_X,\mu_o,\sigma_o$ = parameters of the transformed bivariate normal distribution $f^{(2)}_{XY}(x,y)$;
μ_Y,σ_Y = mean and standard deviation of the Y vertical distances of storm-center positions with respect to the global coordinate system;
$\rho = \rho_{K'N}$ = correlation coefficient of parameters K' and N;
Φ = storm orientation (assuming elliptical shape); and
Ω = random vector of storm characteristics and location.